

## MULTICHANNEL PHOTOREFRACTIVE LASER ULTRASONIC SENSOR

Ph. Delaye, F. Grappin and G. Roosen

Laboratoire Charles Fabry de l'Institut d'Optique du Centre National de la Recherche Scientifique et de l'Université Paris Sud, Centre Scientifique d'Orsay, Orsay Cedex France

**Abstract:** The use of photorefractive laser ultrasonic sensor for laser ultrasound is now well established. The holographic principle on which it is based allows to register the speckled wavefront issued from the target with highly scattering surfaces and to give it back to create a local oscillator with an adapted wavefront. The imaging properties of holography gives the possibility to work with several illuminated points each imaged on its detector. We can then easily transform the system in a multichannel laser ultrasonic sensor. We present here the experimental implementation and characterization of such a sensor, showing that an uniform detection without crosstalk can be realized between the measurement points, if a properly designed set-up is used.

**Introduction:** The basic principle of the Photorefractive Laser Ultrasonic Sensor [1] is a homodyne detection in which we create a reference beam that is identical to the signal beam whatever its wavefront structure. We send the phase modulated signal beam on the photorefractive crystal with a coherent pump beam (Fig. 1). These beams interfere and create in the material a hologram of the signal beam structure. This hologram is a stationary hologram, as the photorefractive crystal has a rather slow response time compared to the time evolution of the phase modulation. The pump beam diffracts on this hologram as a wave that will propagate in the same direction and with the same wavefront structure than the transmitted beam, but without its phase modulation. This diffracted beam thus acts like a local oscillator in a reference beam interferometer. This mechanism is illustrated in the following expression :

$$E_s(x,t) = e^{-\alpha x/2} \left[ \langle E_s(t) \rangle (e^{\gamma x} - 1) + E_s(t) \right] \quad (1)$$

in which the first term of the right member of the equation is the amplitude of the diffracted beam and the second term is the transmitted signal beam. The diffracted beam has the same spatial structure than the transmitted signal beam  $E_s(t)$  but is sensitive only to the mean value of the amplitude (indicated by brackets that means an average over the response time of the holographic media). Thus the written hologram is stationary and is read by a stationary pump beam what gives a stationary diffracted beam which amplitude depends on the diffraction efficiency of the hologram characterized by a photorefractive gain  $\gamma$  (the absorption  $\alpha$  characterizes the losses of the media of thickness  $x$ ).

Diffracted pump beam and signal beam will then interfere (optimally in quadrature as in an homodyne detection) and give an intensity modulated signal [1]:

$$I_s(x,t) = e^{-\alpha x} I_{s0} \left[ e^{2\gamma x} - 2e^{\gamma x} \sin \gamma'' x \varphi(t) \right] \quad (2)$$

To obtain this expression we consider a phase modulated beam with a phase modulation  $\varphi(t)$  created by an ultrasonic vibration of low amplitude ( $\delta(t) \ll \lambda/2$ ). The photorefractive gain is a complex parameter ( $\gamma = \gamma' + i\gamma''$ ) that renders the spatial displacement of the hologram compared to the illumination pattern (an index modulation in phase with illumination would give a purely imaginary gain). In order to have a linear demodulation the imaginary part  $\gamma''$  of the gain should be non zero, what is equivalent to the quadrature condition in a classical homodyne detection. In usual photorefractive crystal, the gain is purely real ( $\pi/2$  phase shifted index grating), unless an external DC field is applied to the crystal [2].

We can note that the use a dynamic holographic material (such as photorefractive crystals) allows the set-up to adapt to fluctuations of the signal beam slower than the crystal response time, writing a new adapted hologram almost instantaneously. This properties gives the Photorefractive Laser Ultrasonic Sensor a high pass frequency response [3], with a cut-off frequency that is related to the response time of the dynamic holographic material. In the case of the photorefractive materials this response time is controlled by the pump beam power and cut-off

frequency around 10kHz can be obtained giving a system insensitive to the low frequency acoustic vibrations that are usually encountered in industrial environment [4]. This system is now well characterized [5] and is commercially available.

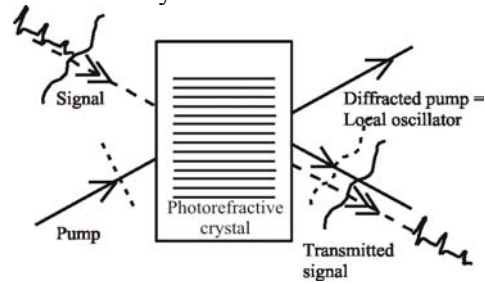


Fig. 1. Schematic principle of the Photorefractive Laser Ultrasonic Sensor

The detection system is usually used with a single detector (even if often in a differential configuration) i.e. that only one measurement point is tested at each laser shot. In usual experimental configurations, the illuminated point on the tested sample is imaged in the photorefractive crystal and imaged again on the photodiode. If we now replace the photodiode by an array or a line of detectors, several detection points can be defined on the target, imaged on the array of detectors and the ultrasonic signal can be measured simultaneously on these multiple points using a single optical system and a single photorefractive crystal [6]. The principle of the multichannel laser ultrasonic sensor thus derives naturally from the Photorefractive Laser Ultrasonic Sensor.

We will present here the implementation of the multichannel laser ultrasonic sensor and an experimental characterization of its performances, regarding the uniformity of the response and the possible crosstalk between the different channels.

**Implementation of the laser ultrasonic sensor:** The first precaution to take, in the implementation of the multichannel sensor, is the illumination of the target. The main parameter that governs the sensitivity of the sensor is the light power collected from the target for a given point [7]. If the laser beam illuminates a large area of the target, the spatial resolution and the position of the tested point on the target will be defined by the detector array. If the detector matrix has a low filling factor (total area of the sensitive zones compared to the total surface of the sensor) a lot of light will be lost by illumination of useless area. The best implementation of such a multichannel sensor will thus require the use of a structured illumination, in the form for example of an array of points of small width and separated by the desired period. This array of illumination points will be then imaged on the detector array, each photodiode receiving light from a well defined area on the target. The resolution is then defined by the size of the illuminating spots, and no more by the photodiode array, and all the light of a single point will be sent on its corresponding photodiode only (in the limit of low inter-spot scattering level).

To generate this array of points we use a diffractive spot array generator (Dammann grating), that generates a 5x5 spot array (Fig. 2A) with a 1mm spacing when placed at the object focal plane of a 63.5mm focal length Fourier lens. The typical diffraction efficiency in each spot was about 3% what gives a total diffraction efficiency around 70%.



Fig. 2 : Image of the array of spots in the target plane (A) and in the detector plane (B) with the dimensions and the position of the photodiode line indicated.

The spot array is then imaged on the scattering target (Fig. 3) using an afocal system lens (all the imaging systems from the first spot array plane to the detector plane are of this type). The typical size of the spots is around  $100\mu\text{m}$  on the target. To extract the scattered reflected light, we used a polarizing beam splitter placed between the afocal lenses and associated with a quarter wave plate placed after the last illuminating lens. All the collected light is reflected by the polarizing beam splitter and sent in the detection direction (light is only slightly depolarized by the sandblasted metallic part). After the polarizing beamsplitter, a second lens makes the image of the illuminated target spot in an intermediate image plane, which is again imaged on the photodiode array (Fig. 2B).

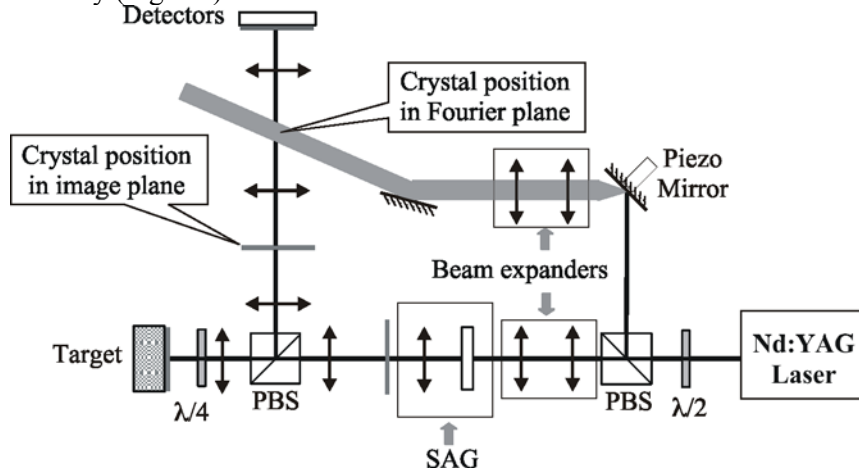


Fig. 3 : Implementation set-up of the multichannel laser ultrasonic sensor. SAG : Spot array generator, PBS : Polarizing beamsplitter

The detector is a line of 16 InGaAs photodiodes with a step of  $0.5\text{mm}$ , and a dimension of the individual elements of  $0.45 \times 1 \text{ mm}^2$ . We choose 5 of these photodiodes to form a 5-detector line with a spacing of  $1\text{mm}$  (Fig. 2B). Each photodiode has its own double stage amplifier (with total transimpedance gain of  $221\text{k}\Omega$ , a cut-off frequency at 3dB of  $800\text{kHz}$  and negligible detector noise). In all the experiments the dominant noise is the intensity noise of the laser. A first experimental characterization of the set-up showed a strong unexpected cross-talk, this cross-talk has been shown to be caused by a light scattering internal to the detector line (10% of the light received by a detector was also detected by the neighboring detector), due to the protection window of the line. The final characterization presented in the following is performed on a detector line in which the protection window had been removed.

The photorefractive crystal is placed in this reflected beam. If we take the example of the Photorefractive Laser Ultrasonic Sensor, the exact position of the photorefractive crystal is of no importance as soon as its aperture is sufficiently large so that it does not stop the light beam. In

the case of the multichannel sensor it should be the same, but in practice there are two preferred positions, in the image plane and in the Fourier plane (i.e. in the common focal plane between the two lenses of the last afocal optical system). Opposite to the single channel case the main properties of the multichannel sensor will depend on the exact position of the crystal, as we will now see.

**Image plane and Fourier plane:** The main characteristics that will be influenced by the position of the crystal are the number of detection points and the sensitivity of the multichannel sensor to crosstalk.

In the Image Plane Architecture (Fig. 4A), the different beams corresponding to the different channels are spatially separated and do not overlap in the photorefractive crystal, leading to completely independent and spatially separated gratings. There is thus no possibilities for them to exchange information, so there will be no crosstalk due to the wave mixing in the holographic media. The drawback is that the number of detected points will be limited by the size of the crystal. Once a system is defined, the addition of spots will be possible to a certain extent until the spot beams do not pass through the crystal anymore and can thus not be detected. We will have to use a large aperture crystal and large dimension of the pump beam to cover the signal beam, what will reduce the power density of the pump beam and thus lead to a slower crystal (as the response time is inversely proportional to the pump beam power density). The demodulation efficiency of the different points will depend on the spatial uniformity of the gain in the crystal (that will depend on the quality of the crystal or on the spatial uniformity of the external applied field).

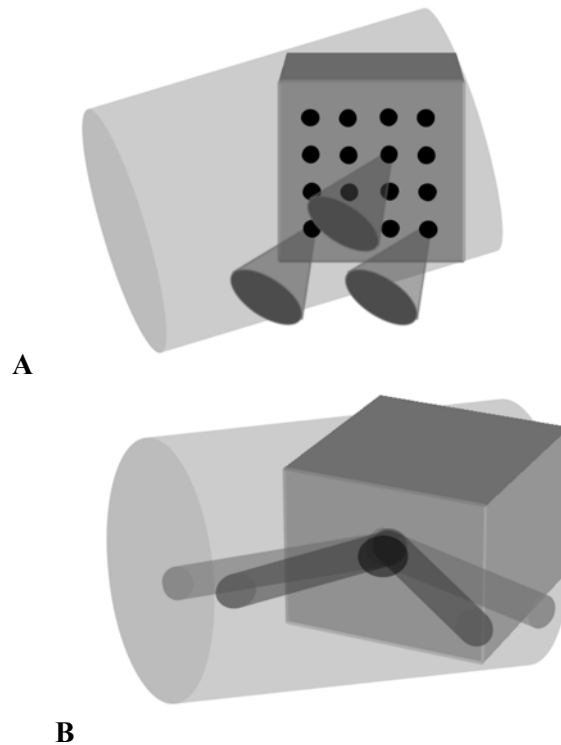


Fig. 4 : Signal beams and pump beam with crystal in the image plane (A) and in the Fourier plane (B).

In the case of the Fourier Plane Architecture (Fig. 4B), the beams arriving from the different spots correspond to collimated beams with varying incidences that overlap in the crystal. This means that all the gratings are written in a single area of the crystal, what might give rise to some exchange between the beams and may lead to crosstalk. The addition of detection spots will not increase the dimension of the interaction area and the dimension of the required crystal, that thus

can be chosen smaller than in the case of the image plane architecture. There will be nevertheless limitations in the number of accessible spots. In this architecture, the diversity of incidence angles of the spots leads to a large variation of the spacing of the gratings written between the pump beam and the signal beams, and thus to a great variation of the efficiency of the written gratings and possibly to a very small demodulation efficiency of the ultrasonic signal for beams arriving with large angles (i.e. the more external spots).

**Origin of the crosstalk:** The crosstalk in the Fourier plane architecture has its origin in the gratings written between the different signal beams that all cross and interact in the crystal. This phenomenon is illustrated in the case of two signal beams in Figure 5. In addition to the gratings written between  $S_1$  or  $S_2$  and the pump  $P$ , the interference of signal beams  $S_1$  and  $S_2$  writes a grating (grating period  $\Lambda_{12}$ ). In the direction of transmitted beam  $S_1$  there is besides the diffracted pump beam, the diffracted  $S_2$  beam that has the same wavefront than  $S_1$  and that carries the phase information from the  $S_2$  beam, leading to possible crosstalk.

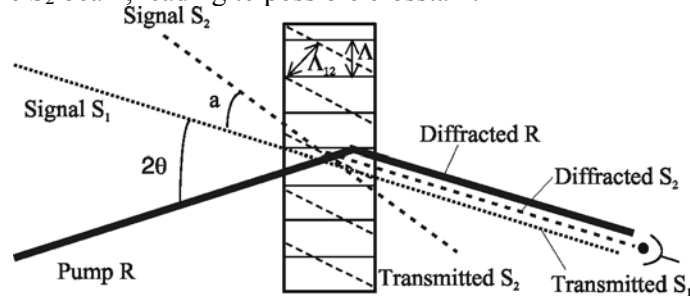


Fig. 5. Origin of the crosstalk in the Fourier plane architecture.

In the general case, the relation (1) will be rewritten in the case of the multichannel sensor in the Fourier plane configuration (to simplify the study we have considered the case of low absorption and low efficiency of the grating, i.e.  $e^{-\alpha x/2} \approx 1$  and  $e^{\gamma x} - 1 \approx \gamma x$ ), for each signal beam  $S_i$  of amplitude  $A_{S_i}$ :

$$A_{S_i}(x, t) = A_{S_i}(0) e^{i\phi_i(t)} + \sum_{j \neq i} \gamma_{S_i S_j} x \cdot A_{S_j}(0) \frac{I_{S_i}}{I_R + \sum_j I_{S_j}} e^{i\phi_j(t)} + \gamma_{RS_i} x \cdot A_{S_i}(0) \frac{I_R}{I_R + \sum_j I_{S_j}} \quad (3)$$

The first term is still the transmitted signal beam, whereas the last term is the reference beam due to the diffraction of the pump beam on the grating it has created by interfering with the signal beam considered. In this term the reduction of the modulation of the interference pattern due to the presence of all the other signal beams has been taken into account (the total incident intensity being  $I_T = I_R + \sum I_{S_j}$  instead of  $I_T = I_R + I_S \approx I_R$  in the single channel case). The additional terms responsible from the crosstalk are the terms in the middle of the expression (3). It deals with the diffraction of the other signal beams  $S_i$  on the gratings they create by their interference with the considered signal beam, the phase present on those beams being transferred on a beam that has a wavefront structure identical to the one of that signal beam as illustrated by the  $A_{S_i}(0)$  amplitude in these terms.

Expression (3) gives us the origin of the cross-talk in the Fourier plane configuration, but it also gives us hints to experimentally reduce this crosstalk. The first way of reduction is to play with the respective intensity of the pump beam and the signal beams. If we have  $I_R + \sum I_{S_j} \gg I_{S_i}$ , what should be relatively easy to obtain as soon as the number of spots will be large, then the crosstalk becomes negligible. To obtain a final expression similar to relation (1) we should also have  $I_R \gg \sum I_{S_j}$  in the last term, to minimize the reduction of the diffraction efficiency due to the presence of the multiple signal beams. The choice of a high power pump beam is thus the best

solution, especially if we note that the first constraint is automatically fulfilled if the second one is verified.

Nevertheless, if it is not possible to fulfill such a condition another parameter on which we can play is the gain  $\gamma_{s,s_i}$  associated with the different parasitic gratings. For example, for a line of spot placed in the vertical plane the inter-signal grating vectors would be perpendicular to the applied electric field and would not benefit of its influence. In the same ways the amplitude of the grating being dependant on the crystal and polarization orientation, it is possible to find architectures for which most of the inter signal grating have reduced or even zero gain.

**Experimental characterization of the multichannel laser ultrasonic sensor:** We implement the multichannel laser ultrasonic sensor and characterize its performances. The laser source is a high power single frequency Nd:YAG laser (power 2.5W) and we place the photorefractive InP:Fe crystal [8] in the image plane. The half angle between the pump beam and the signal beams is around  $17^\circ$  what leads to a mean grating spacing of about  $1.8\mu\text{m}$ . The crystal is used in the "direct detection" configuration [9] with an applied DC field (5kV voltage, corresponding to a  $6900\text{ V}\cdot\text{cm}^{-1}$  applied field), the beam being vertically polarized. In that case, the signal beam intensity at the output of the crystal is given by relation (2). A calibrated piezo-mirror (73.5mrad RMS amplitude at 97.5kHz) is placed on the pump beam. It is used to measure the photorefractive gain ( $\gamma'$  and  $\gamma''$ ), as a response to the known phase modulation (using the fact that the system is sensitive to the phase difference between the two incident beams, meaning that the phase modulation can be put either on the signal beam or the pump beam). The interest of the modulation application to the reference beam is that in the multichannel set-up an identical phase modulation is applied on all the spots, and we have thus access to a map of the photorefractive gain (Fig. 6) seen by the different spots. The gain is uniform between the different points except for a small variation along the line (i.e. parallel to the applied field) certainly due to a residual screening of the applied field due to the pump beam intensity variation on the aperture of the crystal [9]. With these gain and demodulation efficiency, the noise level (governed by the intensity noise of the laser) corresponds to an average value of the minimum measurable displacement around 0.3nm for the different spots. This value is obtained for a typical detected signal of 800mV, that correspond to a detected intensity of  $5,2\mu\text{W}$  (corresponding to an typical incident intensity of  $26\mu\text{W}$ ). Taking into account the detection bandwidth of 800kHz, this gives a normalized detection limit for single shot detection of  $3.4 \times 10^{-6} \text{nm}\sqrt{\text{W}/\text{Hz}}$  (obtained in multiplying the minimum displacement by 2 to take into account the averaging used in the measurement).

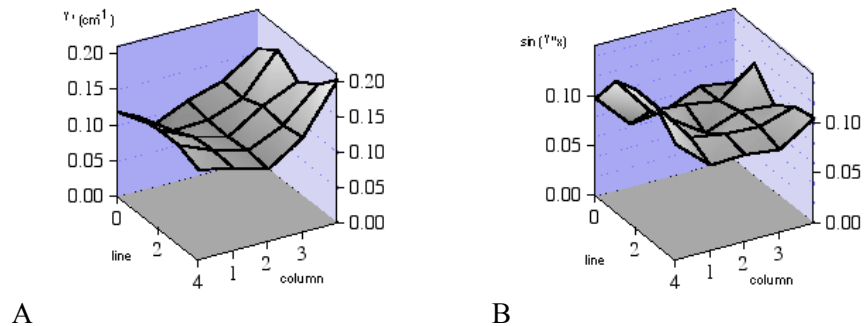


Fig. 6 : Map of the photorefractive gain on the different tested spots, A : the real part of the gain  $\gamma'$ , B the value of the demodulation efficiency  $\sin(\gamma''x)$ . The points are at the line intersections and where all obtained with an average over 4 shots.

The theoretical expression for this detection limit is (supposing a photon noise limited measurement) [1,5] :

$$\delta_{\text{lim}} = \frac{\lambda}{4\pi} \sqrt{\frac{h\nu}{2\eta}} \frac{e^{\alpha x/2}}{\sin \gamma'' x} \quad (4)$$

This gives, with  $e^{\alpha x/2} = 2.23$  for the used crystal, a typical value of  $\sin \gamma'' x = 0.09$  and using  $\eta = 0.9$  for the InGaAs detector at  $1.06 \mu\text{m}$  a theoretical value of  $6.8 \times 10^{-7} \text{nm} \sqrt{\text{W/Hz}}$ . This value is 5 times smaller than the experimental one, mainly due to the residual intensity noise of the laser that is particularly important in the frequency range used in the study and that is not perfectly eliminated by the noise reduction function of the laser. Taking into account this point we have a rather good accordance between experimental results and theory.

The obtained value of the detection limit is correct but far from being optimized, it is nevertheless sufficient for the characterization the other important parameter of the multichannel sensor : the cross-talk.

**Cross-talk evaluation:** For this measurement we use an unknown target, which displacement is measured in the multichannel configuration and compared to the same measurement in the single channel set-up. The target is a plate mounted on a piezoceramic (excited at 97.5kHz). Part of the spots are incident on the vibrating plate and some points illuminate the fixed mount of the plate (Fig. 7A).

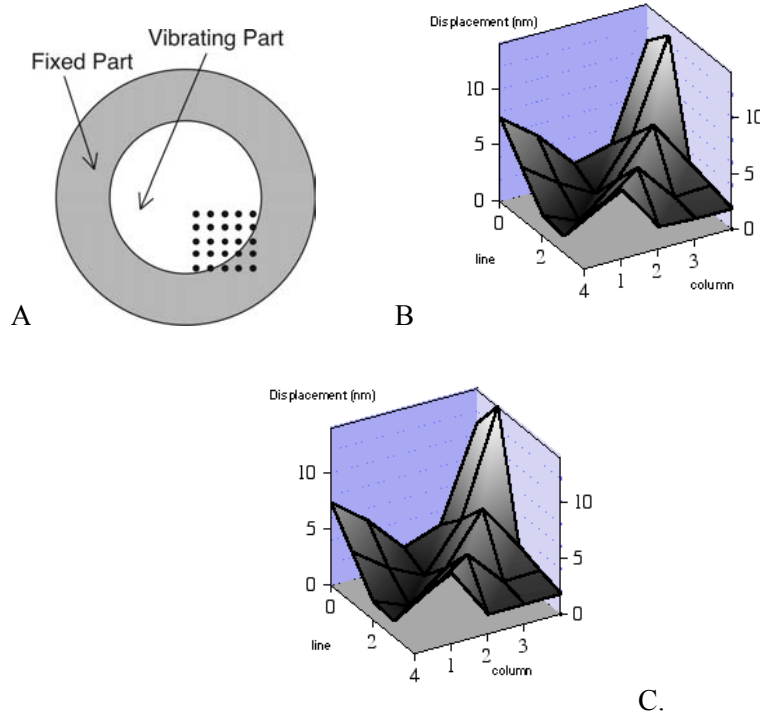


Fig. 7 : A : Scheme of the target with the illuminating spots. B : Displacement of the target in the single channel configuration. C : Displacement of the target in the multichannel configuration.

For the cross-talk characterization, we first perform a reference measurement of the displacement of the target (we use expression (2) with the now known value of the gain  $\gamma$  (Fig. 6) and the phase modulation as the unknown parameter to be determined). For this measurement, only one point illuminates the target for a given measurement and we are thus in the single channel configuration. The point is selected and changed using a square variable diaphragma. The results are shown on the Fig. 7B, where we see the displacement amplitude of the plate with an antinode in the external part of the plate and a vibration node more in the center. Concerning the spots

incident on the fixed mount, the measure gives a small vibration signal due to some residual transfer of vibration from the piezoceramic (that is fixed on that mount).

Once this reference measurement performed, we make the same characterization but in the multichannel configuration, with all the points illuminating the target and a simultaneous measurement on all the detectors of the line (that is then shifted to obtain all the points of the array). The displacement map (Fig. 7C) is similar to the one obtained in the single channel configuration, indicating a low amount of cross-talk. To analyze more quantitatively this cross-talk, we calculate for each point the difference between the two maps, and compare it to the noise level. The results are shown in Table 1. All the measured value are negative indicating a difference between the two maps smaller than the noise level of the measurement, i.e. non significative. Only three points show a positive value and only one of these points show a significative value of the cross-talk (i.e. greater than 100%).

Cross-talk	Col. 0	Col. 1	Col. 2	Col. 3	Col. 4	Intensity	Col. 0	Col. 1	Col. 2	Col. 3	Col. 4
Line 0	-99 %	-66 %	-88 %	-16 %	-18 %	Line 0	587.6	1519	1036	439.4	1372
Line 1	-79 %	-83 %	-25 %	-97 %	273 %	Line 1	302.8	375.5	609.5	1049	483.7
Line 2	-86 %	-86 %	53 %	-94 %	-46 %	Line 2	386.8	1326	862.7	550	1866
Line 3	-98 %	-46 %	8 %	-82 %	-27 %	Line 3	407.3	686.6	566	575.4	828.3
Line 4	-85 %	-61 %	-15 %	-74 %	-97 %	Line 4	687.1	822.3	531.9	687.9	713.2

Table 1 : Map of the crosstalk between the different spots (left table), and the corresponding received intensities (right table).

This point with high cross-talk is rather peculiar as it possesses a rather low intensity (483.7mV detected) and is surrounded by three points of high intensity (2 to 3 times higher mean signal), especially the points above and below, that give more scattered light due to the rectangular shape of the detector (0.45mm X 1mm). Even with the low residual level of scattered light of the optical system (around 1-2% in the horizontal direction) the accumulation of scattered light from these three high intensity points can become important in proportion of the intensity of the considered beam. We reach with this point the limit of the system considering cross-talk, that is light scattering inside the optical system that will have to be reduced to minimum, but that will certainly always stay a problem for a dark points of the target positionned close to bright point for which, even minor scattering may be large compared to the dark spot intensity.

**Conclusions:** We have presented the implementation and characterization of a Multichannel Photorefractive Sensor, that allows simultaneous detection of several ultrasonic signals with a single detection system. A proper implementation of the system is necessary to reduce at maximum the cross-talk between measurement points. The experimental characterization shows that the principle of the detection based on holography does not bring any unexpected cross-talk in a configuration where we should not have any. This configuration in which the spots are imaged in the holographic materials requires a large aperture crystal, and can only with difficulty accept a large number of points (larger than the 5x5 matrix we use). Another configuration can be implemented in which the crystal is placed in the Fourier plane of the spot array. This configuration may be subject to cross-talk as the channels interact in a common area in the crystal, but this crosstalk should be reduced in normal operation of the sensor. This configuration will be tested in future works.

**Acknowledgements:** This work was performed in the frame of the E.C. funded GROWTH project "INCA" (contract G4RD-CT-2001-00507).

**References:**

1. P. Delaye, A. Blouin, D. Drolet, L.A. de Montmorillon, G. Roosen, J.P. Monchalin, "Detection of ultrasonic motion of a scattering surface by photorefractive InP:Fe under an applied dc field." *J. Opt. Soc. Am. B* **14** 1723-34 (1997).
2. L.A. de Montmorillon, Ph. Delaye, J.C. Launay, G. Roosen, "Novel theoretical aspects on photorefractive ultrasonic detection and implementation of a sensor with an optimum", *J. Appl. Phys.* **82**, 5913-22 (1997).
3. Ph. Delaye, L.A. de Montmorillon, G. Roosen, "Transmission of time modulated optical signals through an absorbing photorefractive crystal", *Opt. Commun.* **118**, 154-64 (1995).
4. B. Campagne, A. Blouin, L. Pujol, J.P. Monchalin, "Compact and fast ultrasonic detection device based on two-wave mixing in a gallium arsenide photorefractive crystal" *Rev. Sci. Instrum.* **72**, 2478-82 (2001)
5. L.A. de Montmorillon, P.Delaye, G.Roosen "Photorefractive interferometer for ultrasound detection" in *Progress in Photorefractive nonlinear optics*, K. Kuroda, ed. (Taylor & Francis, London) 213-82 (2002).
6. T.W. Murray, S. Krishnaswamy "Multiplexed interferometer for ultrasonic imaging applications." *Opt. Eng.* **40** 1321-28 (2001)
7. J.-P. Monchalin, "Optical detection of ultrasound", *IEEE Trans. Sonics, Ultrasonics, Freq. Control*, UFFC-**33**, 485-99 (1986).
8. Ph. Delaye, P.U. Halter, G. Roosen. "Continuous-wave two beam coupling in InP:Fe and GaAs : evidence for thermal hole-electron competition in InP:Fe". *J. Opt. Soc. Am. B* **7** 2268-73 (1990).
9. S. de Rossi, Ph. Delaye, G. Roosen, J.C. Launay. "Implementation and comparative evaluation of various architectures of ultrasonic photorefractive sensors" *Optical Materials* **18** 45-48 (2001).